Estimating the impact of influenza on the epidemiological dynamics of SARS-CoV-2

Matthieu Domenech de Cellès [Corresp., 1] , **Jean-Sébastien Casalegno** [2, 3] , **Bruno Lina** [2, 3] , **Lulla Opatowski** [4, 5]

[1] Infectious Disease Epidemiology Group, Max Planck Institute for Infection Biology, Berlin, Germany

[2] Laboratoire de Virologie des HCL, IAI, CNR des virus à transmission respiratoire (dont la grippe) Hôpital de la Croix-Rousse F-69317 Lyon cedex 04, France, Lyon, France

[3] Virpath, Centre International de Recherche en Infectiologie (CIRI), Université de Lyon Inserm U1111, CNRS UMR 5308, ENS de Lyon, UCBL F-69372, Lyon, France

[4] Université Paris-Saclay, UVSQ, Univ. Paris-Sud, Inserm, CESP, Anti-infective evasion and pharma- coepidemiology team, Montigny-Le-Bretonneux, France

[5] Institut Pasteur, Epidemiology and Modelling of Evasion to Antibiotics, Paris, France

Corresponding Author: Matthieu Domenech de Cellès
Email address: domenech@mpiib-berlin.mpg.de

As in past pandemics, co-circulating pathogens may play a role in the epidemiology of coronavirus disease 2019 (COVID-19), caused by the novel severe acute respiratory syndrome coronavirus 2 (SARS-CoV-2). In particular, experimental evidence indicates that influenza infection can up-regulate the expression of ACE2—the receptor of SARS-CoV-2 in human cells—and facilitate SARS-CoV-2 infection. Here we hypothesized that influenza impacted the epidemiology of SARS-CoV-2 during the early 2020 epidemic of COVID-19 in Europe. To test this hypothesis, we developed a population-based model of SARS-CoV-2 transmission and of COVID-19 mortality, which simultaneously incorporated the impact of non-pharmaceutical control measures and of influenza on the epidemiological dynamics of SARS-CoV-2. Using statistical inference methods based on iterated filtering, we confronted this model with mortality incidence data in four European countries (Belgium, Italy, Norway, and Spain) to systematically test a range of assumptions about the impact of influenza. We found consistent evidence for a 1.8–3.4-fold (uncertainty range across countries: 1.1 to 5.0) average population-level increase in SARS-CoV-2 transmission associated with influenza during the period of co-circulation. These estimates remained robust to a variety of alternative assumptions regarding the epidemiological traits of SARS-CoV-2 and the modeled impact of control measures. Although further confirmatory evidence is required, our results suggest that influenza could facilitate the spread and hamper effective control of SARS-CoV-2. More generally, our results highlight the possible role of co-circulating pathogens in the epidemiology of COVID-19.

1 **Estimating the impact of influenza on the epidemiological dynamics of SARS-CoV-2**

2 Matthieu Domenech de Cellès[1, *], Jean-Sébastien Casalegno[2,3],

3 Bruno Lina[2,3], Lulla Opatowski[4,5]

4 1. Max Planck Institute for Infection Biology, Infectious Disease Epidemiology group,

5 Charitéplatz 1, Campus Charité Mitte, 10117 Berlin, Germany

6 2. Laboratoire de Virologie des HCL, IAI, CNR des virus à transmission respiratoire (dont la

7 grippe) Hôpital de la Croix-Rousse F-69317 Lyon cedex 04, France

8 3. Virpath, Centre International de Recherche en Infectiologie (CIRI), Université de Lyon

9 Inserm U1111, CNRS UMR 5308, ENS de Lyon, UCBL F-69372 Lyon cedex 08, France

10 4. Université Paris-Saclay, UVSQ, Univ. Paris-Sud, Inserm, CESP, Anti-infective evasion and

11 pharmacoepidemiology team, F-78180 Montigny-Le-Bretonneux, France

12 5. Institut Pasteur, Epidemiology and Modelling of Evasion to Antibiotics F-75015 Paris,

13 France

14 *Corresponding author:

15 Dr. Matthieu Domenech de Cellès, Max Planck Institute for Infection Biology, Charitéplatz 1,

16 Campus Charité Mitte, 10117 Berlin, Germany. E-mail address: domenech@mpiib-

17 berlin.mpg.de

18 Keywords

19 SARS-CoV-2; COVID-19; influenza; virus-virus interaction; mathematical modeling

20   **Abstract**

21   As in past pandemics, co-circulating pathogens may play a role in the epidemiology of

22   coronavirus disease 2019 (COVID-19), caused by the novel severe acute respiratory syndrome

23   coronavirus 2 (SARS-CoV-2). In particular, experimental evidence indicates that influenza

24   infection can up-regulate the expression of ACE2—the receptor of SARS-CoV-2 in human

25   cells—and facilitate SARS-CoV-2 infection. Here we hypothesized that influenza impacted the

26   epidemiology of SARS-CoV-2 during the early 2020 epidemic of COVID-19 in Europe. To test

27   this hypothesis, we developed a population-based model of SARS-CoV-2 transmission and of

28   COVID-19 mortality, which simultaneously incorporated the impact of non-pharmaceutical

29   control measures and of influenza on the epidemiological dynamics of SARS-CoV-2. Using

30   statistical inference methods based on iterated filtering, we confronted this model with mortality

31   incidence data in four European countries (Belgium, Italy, Norway, and Spain) to systematically

32   test a range of assumptions about the impact of influenza. We found consistent evidence for a

33   1.8–3.4-fold (uncertainty range across countries: 1.1 to 5.0) average population-level increase in

34   SARS-CoV-2 transmission associated with influenza during the period of co-circulation. These

35   estimates remained robust to a variety of alternative assumptions regarding the epidemiological

36   traits of SARS-CoV-2 and the modeled impact of control measures. Although further

37   confirmatory evidence is required, our results suggest that influenza could facilitate the spread

38   and hamper effective control of SARS-CoV-2. More generally, our results highlight the possible

39   role of co-circulating pathogens in the epidemiology of COVID-19.

Introduction

41 The current pandemic of coronavirus disease 2019 (COVID-19), caused by the novel severe

42 acute respiratory syndrome coronavirus 2 (SARS-CoV-2), has led to global alarm. Following the

43 first case reports in December 2019 in Wuhan, China [1], SARS-CoV-2 rapidly spread across the

44 globe and has resulted in approximately 171 million cases and 3.6 million deaths worldwide, as

45 of June 1, 2021 [2]. Because of the initial lack of prophylactic or therapeutic treatments, the

46 pandemic caused the implementation of unprecedented control measures, which culminated in

47 the lockdown of several billion people in over 100 countries during April–May 2020 [3].

48 Although a number of fixed (e.g., greater age, male sex) and chronic (e.g., hypertension,

49 diabetes) risk factors of mortality have now been identified [4], the time-varying drivers of

50 COVID-19 epidemiology remain poorly understood. Experience gained from past pandemics has

51 highlighted the potentially large contribution of co-circulating pathogens to the burden of an

52 emerging disease [5]. Despite the relevance for epidemic forecasting and for designing control

53 strategies, the impact of co-circulating pathogens on SARS-CoV-2 epidemiology has remained

54 largely unexplored [6].

55 Respiratory viruses—including SARS-CoV-2 and other coronaviruses, rhinoviruses,

56 influenza viruses, etc.—form a large class of viruses that cause seasonal infections of the

57 respiratory tract in humans. Mounting evidence indicates that their epidemiologies are not

58 independent, as a result of interaction mechanisms that may operate at different scales and that

59 can be classified as either facilitatory or antagonistic [7,8]. The interaction between the

60 respiratory syncytial virus (RSV) and influenza may provide an example of antagonism. Indeed,

61 experimental evidence in ferrets has shown that influenza viruses induce an antiviral state that

62 transiently limits secondary infection with RSV [9], an effect postulated to explain the delayed

63   epidemic of RSV during the 2009 influenza pandemic [10,11]. Although such antagonistic

64   interactions appear, to date, to be the most common among respiratory viruses [8], experimental

65   evidence indicates that co-infections may have a facilitatory effect, for example by increasing

66   viral growth [12]. Increased transmission of influenza during co-infection with other respiratory

67   viruses was also proposed to explain the multiple waves during the 1918 influenza

68   pandemic [13]. Interestingly, according to recent evidence a viral respiratory infection (in

69   particular with influenza viruses) can up-regulate the expression of ACE2—the cognate receptor

70   of SARS-CoV-2 in human cells—in the respiratory epithelium [14,15]. In addition, this up-

71   regulation was demonstrated experimentally to increase infectivity of SARS-CoV-2 in mice co-

72   infected with influenza A virus [16]. This suggests that respiratory viruses could affect the

73   epidemiology of SARS-CoV-2. Here, we hypothesized that influenza—which peaked in

74   February 2020 and therefore co-circulated during the early spread of COVID-19 in Europe

75   (Fig. 1B)—interacted with SARS-CoV-2.

76   To test this hypothesis, we developed a semi-mechanistic, population-based model of

77   SARS-CoV-2 transmission and of COVID-19 mortality. Using likelihood-based statistical

78   inference methods, we confronted this model to mortality incidence data in four European

79   countries to test a range of assumptions about the impact of influenza on the transmission

80   dynamics of SARS-CoV-2. We find that influenza may have transiently increased the

81   transmission of SARS-CoV-2 during the first wave of COVID-19 in Europe. Although further

82   confirmatory evidence is required, our results suggest that influenza could facilitate the spread of

83   SARS-CoV-2 and, more generally, emphasize the potential role of co-circulating pathogens in

84   the epidemiology of COVID-19.

Materials & Methods

Data

Stringency index data

Country-level time series of the stringency index were available from the Oxford COVID-19 Government Response Tracker, developed at the University of Oxford and described elsewhere [3]. Briefly, the stringency index provides an aggregate measure of the number and of the strictness of non-pharmaceutical control measures implemented by governments in response to the COVID-19 epidemic. The stringency index is defined as the average of 9 normalized ordinal variables, which quantify the strength (e.g., recommended or required) and the scope (e.g., targeted or general) of closure and containment measures (8 variables) and of health measures (1 variable). The resulting index allows quantifying the strength of control measures in a systematic way, on a scale ranging from 0 (no interventions) to 100 (maximum number and maximal intensity of control measures). Of note, however, the stringency index does not quantify the impact of control measures, which likely varied across countries [17]. In formulating our model, we therefore modeled the relationship between the stringency index and the relative reduction in SARS-CoV-2 transmission using a non-decreasing function, whose parameters represented the impact of control measures and were estimated from the data.

Influenza incidence data

Virological data on the weekly numbers of samples tested and of samples positive to any influenza virus were available from the FluNet database, compiled by the WHO (Fig. S1A). Parallel syndromic data on the weekly incidence rate of influenza-like illnesses (ILI) were available from the FluID database, also compiled by the WHO (Fig. S1B). These data were

107 deemed high-quality and used in a previous study on influenza forecasting in the countries

108 considered here [18]. The weekly incidence rate of influenza was then calculated as the product

109 of ILI incidence and of the fraction of samples positive to any influenza virus (Fig. 1B). Because

110 the magnitude of influenza incidence thus calculated varied markedly across countries (e.g., as a

111 result of different surveillance systems and case definitions), we rescaled each time series by its

112 average during the period of co-circulation of influenza and SARS-CoV-2 (Fig. 1B). The

113 resulting time series was therefore dimensionless and equalled 1 when influenza incidence

114 equalled its average value during that period.

COVID-19 mortality data

116 Data on the daily number of deaths caused by SARS-CoV-2 (counted by date of death) were

117 available from national public health public institutes, in Belgium (Sciensano [19]), in Italy

118 (*Dipartimento della Protezione Civile* [20]), and in Spain (*Instituto de Salud Carlos III*, official

119 data with historical corrections compiled by the media DATADISTA [21]). In Norway, the data

120 were available from the worldwide database compiled by the European Center for Disease

121 Control and Prevention [22]. Following a previous study [17], and to avoid a possible bias caused

122 by the dominance of deaths due to non-locally acquired infections early in the epidemic, we

123 included observed deaths from the date after which the cumulative observed death count

124 exceeded 10. Data points before that date were treated as missing and were assigned a

125 conditional log-likelihood of 0, such that they did not contribute to the overall log-likelihood.

126 The data were not further pre-processed, except in Italy, where a negative death count was

127 reported on 24 June 2020 and was treated as missing and also assigned a log-likelihood of 0.

128   *Transmission model*

129   Model formulation

130   We formulated a variant of the standard Susceptible–Exposed–Infected–Recovered transmission

131   model [23], using the method of stages to allow for a realistic distribution of the latent,

132   infectious, and onset-to-death periods [24,25]. Specifically, we assumed that the latent and

133   infectious periods were Erlang-distributed with shape parameter 2 and mean $1/\sigma = 4$ days and

134   $1/\gamma = 5$ days, respectively [26]. The resulting generation time T_g (i.e., the time from infection of

135   a primary case to transmission to a secondary case) had a mean of 6.5 days and a coefficient of

136   variation of 0.58 (see Fig. S2 for the full distribution and the details of the calculation), consistent

137   with empirical observations and with the values fixed in a previous modeling study [17,27]. To

138   model the impact of the gradual implementation of non-pharmaceutical control measures (e.g.,

139   border closure, school closure, lockdown), we mapped the stringency index (denoted by $si(t)$) to

140   the time-varying relative reduction in transmission of SARS-CoV-2 (denoted by $r_\beta(t)$).

141   Specifically, we used the following simple linear scaling function, with saturation:

142
$$r_\beta(t) = \min(1, b \times \frac{si(t)}{100})$$

143   Here the parameter b quantifies how steeply the transmission rate of SARS-CoV-2 decreases as

144   the stringency index increases. Hence, this parameter can be interpreted as a measure of the

145   impact of non-pharmaceutical control measures on SARS-CoV-2 transmission. The deterministic

146   variant of the model was represented by the following set of differential equations:

147
$$\begin{aligned}
\dot{S} &= -\lambda(t)S \\
\dot{E}_1 &= \lambda(t)S - 2\sigma E_1 \\
\dot{E}_2 &= 2\sigma(E_1 - E_2) \\
\dot{I}_1 &= 2\sigma E_2 - 2\gamma I_1 \\
\dot{I}_2 &= 2\gamma(I_1 - I_2) \\
\dot{R} &= 2\gamma I_2
\end{aligned}$$

148 The force of infection (that is, the per capita rate at which susceptible individuals contract

149 infection [23]), $\lambda(t)$, was modeled as:

150
$$\begin{aligned}
\lambda(t) &= \beta(t)\frac{I_1 + I_2}{N} \\
\beta(t) &= \beta_0(1 - r_\beta(t))\beta_F(t) \\
r_\beta(t) &= \min(1, b \times \frac{si(t)}{100}) \\
\beta_F(t) &= \max(0, 1 + \beta_F F(t)) \\
R_e(t) &= \frac{\beta(t)}{\gamma} \times \frac{S(t)}{N}
\end{aligned}$$

151 where R_0 represents the basic reproduction number of SARS-CoV-2, $\beta_0 = R_0\gamma$ the basic

152 transmission rate, $R_e(t)$ the time-varying effective reproduction number, N the population size

153 (assumed constant during the study period), and $F(t)$ the renormalized time series of influenza

154 incidence, incorporated as a covariate into the model (Fig. 1). With this formulation, the

155 parameter β_F quantifies the impact of influenza on SARS-CoV-2 transmission: $\beta_F > 0$ if

156 influenza increases transmission, $\beta_F < 0$ if influenza decreases transmission, and $\beta_F = 0$ if

157 influenza has no impact on transmission (null hypothesis). More specifically, the average

158 incidence of influenza during the period of co-circulation with SARS-CoV-2 corresponds to

159 $F(t) = 1$, such that $1 + \beta_F$ represents the average relative variation of SARS-CoV-

160 2 transmission associated with influenza. In writing the equations, we implicitly assume that the

161   impact of influenza on SARS-CoV-2 transmission, if any, is short-lived and does not extend long

162   after influenza infection.

163   Finally, we incorporated an observation model that related the dynamics of SARS-CoV-

164   2 infection to that of COVID-19 mortality, taking into account the fact that only a fraction of

165   infections results in death and that, among those, death occurs some time after symptom

166   onset [17,28,29]. We assumed an average duration of pre-symptomatic of 2.5 days, resulting in

167   an average incubation period of 6.5 days, in broad agreement with previous empirical

168   studies [29,30]. Hence, individuals in the first infected state (I_1) were considered pre-

169   symptomatic, and the onset of symptoms was assumed to coincide with the transition from I_1 to

170   I_2. The onset-to-death time was then assumed to be Erlang distributed with shape parameter 5

171   and mean $1/\kappa = 17.8$ days (coefficient of variation of 0.45), the value estimated in a previous

172   epidemiological study [28]. In a sensitivity analysis, we also tested a mean onset-to-death time of

173    $1/\kappa = 13$ days, the lower bound estimated in a meta-analysis [29]. According to previous studies

174   in European countries, the infection fatality ratio (IFR) typically ranged from 0.5% to 1% early

175   in the epidemic [31–33]. We fixed the IFR to $\mu = 0.01$ in the base model, but we considered an

176   alternative value of 0.005 in a sensitivity analysis. Given those assumptions, the observation

177   model was modeled by the following set of ordinary differential equations:

178
$$\begin{aligned} \dot{Q}_1 &= 2\gamma\mu I_1 - 5\kappa Q_1 \\ \dot{Q}_{i=2,\ldots,5} &= 5\kappa(Q_{i-1} - Q_i) \\ \dot{D}_M &= 5\kappa Q_5 \end{aligned}$$

179   Here D_M is the simulated number of daily deaths, modeled as an accumulator variable and reset

180   to 0 at the end of each day. The observed number of daily deaths, D_O, was modeled using a

181   negative binomial distribution with mean D_M and over-dispersion k_D (i.e., $\mathbb{V}(D_O|D_M) = D_M + k_D$

182   D_M^2), a standard distribution used in previous modeling studies [17,34].

183   As in Flaxman et al. [17], simulations were started 30 days before the date from which

184   the cumulative observed death count first exceeded 10. At that date, we assumed that $E_1(0)$

185   individuals had been exposed to SARS-CoV-2; other individuals were assumed susceptible to

186   infection (i.e., $S(0) = N - E_1(0)$), and all other compartments were initialized to 0.

187   Stochastic variant and modeling of superspreading

188   The stochastic variant of the model was implemented as a continuous-time Markov process

189   approximated via a multinomial modification of the τ-leap algorithm [35], with a fixed time step

190   of $\Delta t = 10^{-1}$ day. To model the effect of superspreading events—a key feature of SARS-CoV-

191   2 transmission dynamics [36]—, extra-demographic stochasticity was added to the transmission

192   rate $\beta(t)$. Specifically, as proposed by Kain et al. [37], at every time step we drew a value of β_0

193   from a Gamma white noise distribution:

194
$$\beta_0 \sim \Gamma_{\text{WN}}\left(\sigma = \sqrt{\frac{R_0}{(I_1 + I_2)k\Delta t}}, \mu = R_0\gamma\right)$$

195   with mean μ and variance $\mu\sigma^2$. Here k represents the dispersion parameter of the Negative-

196   binomial distribution for the individual reproduction number (with mean R_0 and variance $R_0 + \frac{R_0^2}{k}$

197   ), as estimated in previous studies [38,39]. As in [37] and in keeping with empirical estimates

198   from contact tracing studies of SARS-CoV-2 [39], we fixed $k = 0.16$.

199 Model estimation

200 Following the method presented in[17], we estimated unknown model parameters using observed

201 COVID-19 mortality data alone. Indeed, because of the initially limited testing capacity

202 (typically reserved to severe cases or high-risk groups), mortality data were arguably more

203 reliable than case data early in the epidemic in most countries [17]. By incorporating known

204 epidemiological parameters (key among those the onset-to-death time, the IFR, and the

205 generation time), however, the method allows back-calculating infection rates from observed

206 death rates. Hence, in addition to the dynamic of mortality, we also reconstructed the dynamic of

207 infection and, as a validation, compared it to external epidemiological data—like cross-sectional

208 seroprevalence estimates—when available.

209   The following five parameters were estimated from the data:

210 1. The basic reproduction number, R_0. According to a previous meta-analysis [40], this

211   parameter was searched in the interval 1–10.

212 2. The impact of non-pharmaceutical control measures, b. The lower bound of the search

213   interval of this parameter was fixed to 0.5, such that the maximal value of the stringency

214   index ($s = 100$) corresponded to a minimal reduction of SARS-CoV-2 transmission of

215   50% [17].

216 3. The impact of influenza on SARS-CoV-2 transmission, β_F (search interval: $\mathbb{R}$).

217 4. The initial number of individuals exposed to SARS-CoV-2, $E_1(0)$ (search interval: 0–10^4).

218 5. The over-dispersion in death reporting, k_D (search interval: $\mathbb{R}^+$).

219   A summary list of fixed and estimated model parameters is presented in Table 1.

220   All parameters were transformed to be estimated on the real line, using a log

221   transformation for positive parameters and the extended logistic function $f(\theta) = \log\frac{\theta - a}{b - \theta}$ for

222   parameters constrained in the interval $[a,b]$. The maximum iterated filtering algorithm

223   (MIF2 [41]), implemented in the R (version 3.6.3) package pomp [42,43] (version 2.7), was used

224   to estimate model parameters. The R checkpoint package was used to freeze all the packages'

225   version at the date of April 3, 2020 [44]. The estimation was completed in several steps, starting

226   with trajectory matching to identify good starting parameters for MIF2, followed by 100

227   independent runs of MIF2 to locate the maximum likelihood estimate (MLE). Each MIF run had

228   150 iterations with 5,000 particles, geometric cooling, and a random walk standard deviation of

229   0.1 for the initial condition $E_1(0)$ and of 0.02 for the other parameters. The log-likelihood of

230   every parameter set was calculated as the log of the mean likelihood of 5 replicate particle filters,

231   each with 20,000 particles. The profile likelihood was calculated to verify the convergence of

232   MIF2 and to derive an approximate 95% confidence interval for the parameter β_F [45]—the

233   parameter of key interest in our study. For the other parameters, a parametric bootstrap was used

234   to calculate approximate 95% confidence intervals, by re-estimating the parameters for each of

235   200 synthetic datasets simulated at the MLE [46,47]. Compared with the profile likelihood, the

236   parametric bootstrap requires less computation and was found to perform well in previous

237   applications [46, 47].

238

239   Sensitivity analyses

240   To verify the robustness of the parameter estimates, we conducted six sensitivity analyses

241   (further detailed in the Supplementary Results). First, we estimated an extended model in which

242   the reduction of SARS-CoV-2 transmission was allowed to scale non-linearly with the stringency

243   index. Second, to test the possible presence of other variables confounded with influenza, we

244   estimated a model that included an exponential trend in the transmission rate of SARS-CoV-2.

245   Finally, we varied the fixed value of 3 parameters and re-estimated the parameters of the base

246   model. Specifically, we tested two alternative values of the average generation time ($\mathbb{E}(T_g) = 5$

247   days and $\mathbb{E}(T_g) = 7.5$ days), one alternative value of the infection fatality ratio ($\mu = 0.005$), and

248   one alternative value of the average onset-to-death period ($\frac{1}{\kappa} = 13$ days).

249   **Results**

250   Parameter estimates

251   As shown in Fig. 1A, the number and the intensity of control measures against COVID-

252   19 gradually increased from January until the nationwide lockdown in March, before a relaxation

253   from May 2020. During this time period, the epidemic of influenza started in January 2020 and

254   ended in March 2020, with a peak during February in each country (Fig. 1B and S1). Despite

255   correlations between some parameters (in particular the reproduction number and the impact of

256   control measures, see Fig. S4), all parameters were identifiable in each country (Table 2).

257   Parameter estimates indicated that, during the period of co-circulation, influenza was associated

258   with an average 1.8–3.4-fold (uncertainty range across countries: 1.1 to 5.0) population-level

259   increase in SARS-CoV-2 transmission (Table 2 and Fig. S3). After controlling for the impact of

260   influenza, our estimates of the basic reproduction number (R_0) ranged from 1.2 (in Italy) to 3.4

261 (in Belgium). Although the increased transmission associated with influenza early during the

262 SARS-CoV-2 epidemic explained the data significantly better (Table 2), a model without

263 influenza led to higher R_0 estimates (range 2.4–5.2, Fig. 2A), consistent with those of a previous

264 study [17]. Also in line with [17], we found consistent evidence for a marked impact of non-

265 pharmaceutical control measures (Table 2), which were associated with a decrease in SARS-

266 CoV-2 transmission below the reproduction threshold from mid-March to June 2020 (Fig. 2A).

267 Model evaluation

268 Visual inspection of simulations suggested that our model correctly captured the dynamics of

269 COVID-19 mortality in every country (Fig. 2B). A more detailed model–data comparison of

270 summary statistics confirmed that our model accurately reproduced the peak time, the peak

271 number and the total number of deaths, and the death growth exponent [48], except in Italy and

272 Spain where the latter statistic was systematically under-estimated (Fig. S5). Our model-based

273 estimates of the total proportion of individuals infected with SARS-CoV-2 (as of 4 May 2020,

274 Table 2) were also comparable with those of a previous modeling study [17] and of a

275 seroprevalence study conducted in early May in Spain (approximate seroprevalence estimate of

276 5% [49]). Hence, our model appeared to precisely recapitulate the epidemiology of SARS-CoV-

277 2 morbidity and mortality over a period of $\sim$ 4 months.

278 Sensitivity analyses

279 The results of the sensitivity analyses are presented in Tables S1–S3. We found little statistical

280 evidence that the model with non-linear scaling of the stringency index outperformed the model

281 with simple linear scaling in any country ($\Delta\log L \in [0.0,1.1]$, likelihood ratio test P-value

282 $P \in [0.14,1.00]$, Table S1). Of note, although our estimates of the impact of influenza varied

283   little, the additional estimated parameter resulted in higher parametric uncertainty, particularly in

284   Norway where the approximate 95% CI embraced the null value. Similarly, the model with an

285   unexplained exponential trend in transmission did not substantially improve model fit ($\Delta\log$

286    $L \in [0.0, 3.2]$, likelihood ratio test P-value $P \in [0.01, 1.00]$, Table S2). Despite higher parametric

287   uncertainty caused by the estimation of the trend, our results regarding the impact of influenza

288   remained robust, but once again the approximate confidence interval embraced the null value in

289   Norway. In addition, we found that the parameter estimates varied little when testing alternative

290   hypotheses about the fixed value of the average generation time, of the onset-to-death time, and

291   of the infection fatality ratio (Table S3). Finally, because our R_0 estimates were lower than

292   previous estimates in Italy and Spain, we tested an alternative model with R_0 fixed to 2.5 in each

293   country. This model led to broadly similar conclusions, although the estimated impact of

294   influenza was lower both in Italy ($\beta_F = 1.4$, approximate 95% CI [1.2, 1.5], $\log L = -692.3$

295   [SE<0.1]) and in Spain ($\beta_F = 0.7$, approximate 95% CI [0.4, 1.0], $\log L = -567.7$ [SE=0.1]). In

296   sum, our main result about the impact of influenza remained robust to a variety of alternative

297   assumptions regarding the epidemiological traits of SARS-CoV-2 and the modeled impact of

298   control measures.

Discussion

300   The main goal of this study was to test the hypothesis that influenza impacted the

301   epidemiological dynamics of SARS-CoV-2, building on previous experimental evidence of a

302   positive interaction between the two viruses [14–16]. To do so, we developed a semi-

303   mechanistic, population-based model of SARS-CoV-2 transmission and of COVID-19 mortality,

304   which simultaneously incorporated the impact of non-pharmaceutical control measures and of

305   influenza. Using likelihood-based statistical inference techniques, we confronted this model with

306   mortality incidence data in four European countries to systematically test a range of assumptions

307   about the possible impact of influenza and of control measures. In keeping with previous

308   studies [17], we found robust and consistent evidence that control measures markedly reduced

309   the transmission of SARS-CoV-2. In addition, we also found consistent evidence suggesting that

310   co-circulation of influenza transiently facilitated the transmission of SARS-CoV-2 early in the

311   epidemic in Europe.

312   Our study has a number of important limitations. First, as in other studies [17,26,50] and

313   because of a lack of appropriate age-specific data (for example on the temporal changes in the

314   contact matrix and in the incidence of influenza), our model was not age-structured, even though

315   many aspects of COVID-19 and of influenza epidemiology—like disease severity and

316   lethality—vary markedly with age [28]. The susceptibility to SARS-CoV-2 infection was also

317   found to increase with age [51], a finding potentially explained by lower baseline expression of

318   the ACE2 receptor in children [52]. A testable prediction of our model, therefore, is that

319   influenza should be associated with a transient increase in susceptibility to SARS-CoV-

320   2 infection, commensurate with the variations of influenza incidence over age. Second, we

321   modeled the impact of non-pharmaceutical control measures using a simple, linear function

322   scaling the stringency index to the reduction of SARS-CoV-2 transmission. Even though this

323   simple hypothesis provided a more parsimonious fit (except in Italy), that result may be specific

324   to Europe, where control measures gradually increased in number and in intensity (Fig. 1A). In

325   general, the association is likely non-linear (e.g., if a high-impact intervention like a lockdown is

326   implemented early on), and we therefore recommend testing a variety of scaling functions. More

327   generally, although our model builds on a previously validated method to estimate the time-

328   varying reproduction number [17], we acknowledge that the stringency index may not fully

329   capture temporal variations in SARS-CoV-2 transmission, in particular behavior changes outside

330   of what was mandated by governments. Even though we tested a model with an unexplained

331   trend in transmission (Table S2), more complex temporal functions may be required to fully

332   capture such changes. Third, we did not incorporate climate into our model, even though, as for

333   other respiratory viruses, environmental variables like temperature and humidity may affect the

334   transmission of SARS-CoV-2. According to previous studies conducted in a variety of locations

335   worldwide, however, the impact of weather on the SARS-CoV-2 epidemic appears to have been

336   modest, at least during the first wave in early 2020 [53–55]. These findings are also consistent

337   with epidemiological theory, which predicts that, because of lack of population immunity, the

338   initial pandemic trajectory may be relatively insensitive to climate [56]. Fourth, we did not

339   specifically model fully asymptomatic cases, which may represent a large fraction of SARS-

340   CoV-2 infections [26]. The omission of asymptomatic infections may lead to biased R_0 estimates

341   if their duration significantly differs from that of symptomatic infections [57]. A previous study,

342   however, estimated that the duration of both types of infection is comparable [26], such that our

343   estimates should be robust in more complex model structures. Finally, we assessed only the

344   impact of influenza, because of its high prevalence and period of overlap with SARS-CoV-2 in

345   early 2020 in Europe and of the availability of high-quality data [18]. Nevertheless, other

346   respiratory viruses, like RSV and rhinoviruses [58], may also interact with SARS-CoV-2 and

347   could be considered.

348   Acknowledging these limitations, our model makes at least two other predictions that

349   could be tested to provide confirmatory evidence. First, even though our results did not allow to

350   distinguish between higher transmissibility or higher susceptibility in individuals co-infected

351   with influenza and SARS-CoV-2, previous experimental work suggests that the latter mechanism

352   may operate, as a result of up-regulation of the ACE2 receptor caused by influenza

353   infection [14,15]. Hence, we predict that a recent influenza infection should be an independent

354   risk factor for subsequent SARS-CoV-2 infection. Estimates of the frequency of co-detection of

355   influenza and SARS-CoV-2 by polymerase chain reaction (PCR) testing in nasopharyngeal

356   swabs were highly variable in previous studies (range 0–60% [6,59]). Although the marked

357   seasonality of influenza in temperate regions likely explains in part the low frequency found in

358   some studies [59], we propose that differences in the natural history of influenza and SARS-

359   CoV-2 infections also lead to a systematic under-estimation of co-infection. Specifically, because

360   the incubation period of SARS-CoV-2 infection (estimated to average 5.7 days [29]) exceeds that

361   of influenza (A, 1.4 days or B, 0.6 days [60]), it is likely that, by the time SARS-CoV-2 infection

362   becomes detectable, influenza no longer is. To make that statement more precise, we calculated

363   the probability of detectability of a co-infection, with influenza first then SARS-CoV-

364   2 (Table S4). Assuming that influenza is detectable by PCR up to 4–5 days after [61], and SARS-

365   CoV-2 from 2–4 days before [30], symptom onset, we find that a large fraction (30–50%) of co-

366   infections may not be detectable at all. These results may help explain the low frequency of co-

367   detection found in some studies [62], and suggest that the time window of co-detectability may

368   be too short to adequately infer the association between influenza and SARS-CoV-2 using PCR

369   testing. Serological studies comparing the prevalence of antibodies against influenza in SARS-

370   CoV-2 cases and non-cases may therefore be required to test the prediction that influenza is a

371   risk factor for SARS-CoV-2 infection. Second, we predict that individuals vaccinated against

372   influenza should be at lower risk of SARS-CoV-2 infection than those unvaccinated. The

373   findings of a negative association between influenza vaccine coverage and COVID-19 mortality

374   in ecological studies (in Italy [63] and in other countries [64]) and of a lower risk of SARS-CoV-

375   2 infection in influenza vaccinees in some individual-level epidemiological studies (reviewed

376   in [65]) are consistent with our prediction, but further epidemiological investigations are needed.

377   Importantly, our results can explain these findings as the direct effect of influenza vaccines on

378   influenza infection, instead of indirect effects on non-influenza pathogens (e.g., as a result of

379   trained immunity) [66].

380   With the likely prospect of COVID-19 becoming endemic, the potential interactions of

381   SARS-CoV-2 with other respiratory pathogens—in particular respiratory viruses—may become

382   a key public health issue. In this context, our results suggest that influenza could facilitate the

383   circulation of SARS-CoV-2 and therefore increase the burden of COVID-19. As outlined above,

384   these results are consistent with several lines of experimental [16, 14, 15] and epidemiological

385   [65, 64, 63] evidence. We note, however, that a previous study proposed that influenza and

386   SARS-CoV-2 have competitive interactions [67]. Specifically, using a within- host model of

387   viral replication Pinky and Dobrovolny found that the low growth rate of SARS-CoV-2 may

388   result in limited access to target cells and therefore suppression by other respiratory viruses [67].

389   Although this mechanism may be generally relevant for respiratory viruses, the ability of

390   influenza to up-regulate ACE2 [14, 15]—a feature not included in the within-host model [67]—

391   could counteract this mechanism and explain the increased infectivity of SARS-CoV-2 found

392   experimentally [16]. Of note, in keeping with [67], another experimental study found evidence

393   that the interferon response caused competitive interactions between rhinoviruses and SARS-

394   CoV-2 [58]. Hence, these different biological mechanisms suggest that every respiratory virus

395   interacts with SARS-CoV-2 in a highly specific way, with influenza being unique in its ability to

396   up-regulate ACE2 and to increase SARS-CoV-2 infectivity [16].

397

Conclusions

399 In conclusion, our results suggest that influenza virus infection could have increased the

400 transmission of SARS-CoV-2 and facilitated its spread during the early 2020 epidemic of

401 COVID-19 in Europe. Hence, an increase in the uptake of influenza vaccines may be called for,

402 not only to reduce hospitalizations due to influenza infections [59,68], but also to reduce their

403 downstream impact on SARS-CoV-2 transmission and on COVID-19 mortality. More generally,

404 taking into account the microbial environment of SARS-CoV-2 may be essential, not only to

405 better understand its epidemiology, but also to enhance current and future infection control

406 strategies.

407 **Acknowledgements**

408 Availability of data and materials

409 The data used for this analysis are freely available from the databases cited in the references and

410 have been compiled into a database available from Edmond, the Open Data Repository of the

411 Max Planck Society: https://edmond.mpdl.mpg.de/imeji/collection/eUiBI4vpiGxi4126. The R

412 programming codes to implement and estimate the models are also available on this repository.

413 Competing interests

414 MDdC received postdoctoral funding (2017–2019) from Pfizer and consulting fees from GSK.

415 JSC declares no competing interests. BL is chair of the ISC for the Global Influenza Surveillance

416 Network, and co-chair of the Global Influenza and RSV initiative; he is also a member of the

417 French COVID-19 Scientific Committee (no personal income for all these activities). LO has

418 received consulting fees from WHO for work on antimicrobial resistance and funding from

419 Pfizer (2017–2019).

420 Authors contributions

421 MDdC conceived of the study design and performed the analysis. JSC and BL provided content

422 expertise. LO conceived of the study design and oversaw the analysis.

423 Acknowledgements

424 We thank Arturo Zychlinsky and Klaus Osterrieder for helpful comments on the manuscript.

425 Computations underlying the present analysis were performed at the Max Planck Computing and

426 Data Facility (MPCDF).

427 **References**

428

429 1. Zhu N, Zhang D, Wang W, Li X, Yang B, Song J, Zhao X, Huang B, Shi W, Lu R, Niu P,

430 Zhan F, Ma X, Wang D, Xu W, Wu G, Gao GF, Tan W, and China Novel Coronavirus

431 Investigating and Research Team. 2020. A Novel Coronavirus from Patients with Pneumonia in

432 China, 2019. *N Engl J Med* 382:727-733. 10.1056/NEJMoa2001017

433 2. Johns Hopkins University Center for Systems Science and Engineering (JHU CCSE). Novel

434 coronavirus (covid-19) cases data [Internet]. Available from:

435 https://data.humdata.org/dataset/novel-coronavirus-2019-ncov-cases

436 3. Hale T, Webster S, Petherick A, Phillips T, Kira B. Oxford covid-19 government response

437 tracker. Blavatnik School of Government Working Paper [Internet]. Available from:

438 www.bsg.ox.ac.uk/covidtracker

439 4. Williamson EJ, Walker AJ, Bhaskaran K, Bacon S, Bates C, Morton CE, Curtis HJ, Mehrkar

440 A, Evans D, Inglesby P, Cockburn J, McDonald HI, MacKenna B, Tomlinson L, Douglas IJ,

441 Rentsch CT, Mathur R, Wong AYS, Grieve R, Harrison D, Forbes H, Schultze A, Croker R,

442 Parry J, Hester F, Harper S, Perera R, Evans SJW, Smeeth L, and Goldacre B. 2020. Factors

443 associated with COVID-19-related death using OpenSAFELY. *Nature*. 10.1038/s41586-020-

444 2521-4

445 5. Morens DM, Taubenberger JK, and Fauci AS. 2008. Predominant role of bacterial pneumonia

446 as a cause of death in pandemic influenza: implications for pandemic influenza preparedness. *J*

447 *Infect Dis* 198:962-970. 10.1086/591708

448   6. Thindwa D, Garcia Quesada M, Liu Y, Bennett J, Cohen C, Knoll MD, von Gottberg A,

449   Hayford K, and Flasche S. 2020. Use of seasonal influenza and pneumococcal polysaccharide

450   vaccines in older adults to reduce COVID-19 mortality. *Vaccine* 38:5398-5401.

451   10.1016/j.vaccine.2020.06.047

452   7. DaPalma T, Doonan BP, Trager NM, and Kasman LM. 2010. A systematic approach to virus-

453   virus interactions. *Virus Res* 149:1-9. 10.1016/j.virusres.2010.01.002

454   8. Opatowski L, Baguelin M, and Eggo RM. 2018. Influenza interaction with cocirculating

455   pathogens and its impact on surveillance, pathogenesis, and epidemic profile: A key role for

456   mathematical modelling. *PLoS Pathog* 14:e1006770. 10.1371/journal.ppat.1006770

457   9. Chan KF, Carolan LA, Korenkov D, Druce J, McCaw J, Reading PC, Barr IG, and Laurie KL.

458   2018. Investigating Viral Interference Between Influenza A Virus and Human Respiratory

459   Syncytial Virus in a Ferret Model of Infection. *J Infect Dis* 218:406-417. 10.1093/infdis/jiy184

460   10. Casalegno JS, Ottmann M, Bouscambert-Duchamp M, Valette M, Morfin F, and Lina B.

461   2010. Impact of the 2009 influenza A(H1N1) pandemic wave on the pattern of hibernal

462   respiratory virus epidemics, France, 2009. *Euro Surveill* 15.

463   11. Mak GC, Wong AH, Ho WYY, and Lim W. 2012. The impact of pandemic influenza A

464   (H1N1) 2009 on the circulation of respiratory viruses 2009-2011. *Influenza Other Respir Viruses*

465   6:e6-10. 10.1111/j.1750-2659.2011.00323.x

466   12. Goto H, Ihira H, Morishita K, Tsuchiya M, Ohta K, Yumine N, Tsurudome M, and Nishio

467   M. 2016. Enhanced growth of influenza A virus by coinfection with human parainfluenza virus

468   type 2. *Med Microbiol Immunol* 205:209-218. 10.1007/s00430-015-0441-y

469 13. Merler S, Poletti P, Ajelli M, Caprile B, and Manfredi P. 2008. Coinfection can trigger

470 multiple pandemic waves. *J Theor Biol* 254:499-507. 10.1016/j.jtbi.2008.06.004

471 14. Smith JC, Sausville EL, Girish V, Yuan ML, Vasudevan A, John KM, and Sheltzer JM.

472 2020. Cigarette Smoke Exposure and Inflammatory Signaling Increase the Expression of the

473 SARS-CoV-2 Receptor ACE2 in the Respiratory Tract. *Dev Cell* 53:514-529.e513.

474 10.1016/j.devcel.2020.05.012

475 15. Ziegler CGK, Allon SJ, Nyquist SK, Mbano IM, Miao VN, Tzouanas CN, Cao Y, Yousif

476 AS, Bals J, Hauser BM, Feldman J, Muus C, Wadsworth n, Marc H, Kazer SW, Hughes TK,

477 Doran B, Gatter GJ, Vukovic M, Taliaferro F, Mead BE, Guo Z, Wang JP, Gras D, Plaisant M,

478 Ansari M, Angelidis I, Adler H, Sucre JMS, Taylor CJ, Lin B, Waghray A, Mitsialis V, Dwyer

479 DF, Buchheit KM, Boyce JA, Barrett NA, Laidlaw TM, Carroll SL, Colonna L, Tkachev V,

480 Peterson CW, Yu A, Zheng HB, Gideon HP, Winchell CG, Lin PL, Bingle CD, Snapper SB,

481 Kropski JA, Theis FJ, Schiller HB, Zaragosi L-E, Barbry P, Leslie A, Kiem H-P, Flynn JL,

482 Fortune SM, Berger B, Finberg RW, Kean LS, Garber M, Schmidt AG, Lingwood D, Shalek

483 AK, Ordovas-Montanes J, HCA Lung Biological Network. Electronic address: lung-

484 network@humancellatlas.org, and HCA Lung Biological Network. 2020. SARS-CoV-2

485 Receptor ACE2 Is an Interferon-Stimulated Gene in Human Airway Epithelial Cells and Is

486 Detected in Specific Cell Subsets across Tissues. *Cell* 181:1016-1035.e1019.

487 10.1016/j.cell.2020.04.035

488 16. Bai L, Zhao Y, Dong J, Liang S, Guo M, Liu X, Wang X, Huang Z, Sun X, Zhang Z, Dong

489 L, Liu Q, Zheng Y, Niu D, Xiang M, Song K, Ye J, Zheng W, Tang Z, Tang M, Zhou Y, Shen C,

490   Dai M, Zhou L, Chen Y, Yan H, Lan K, and Xu K. 2021. Coinfection with influenza A virus

491   enhances SARS-CoV-2 infectivity. *Cell Res* 31:395-403. 10.1038/s41422-021-00473-1

492   17. Flaxman S, Mishra S, Gandy A, Unwin HJT, Mellan TA, Coupland H, Whittaker C, Zhu H,

493   Berah T, Eaton JW, Monod M, Imperial College COVID-19 Response Team, Ghani AC,

494   Donnelly CA, Riley SM, Vollmer MAC, Ferguson NM, Okell LC, and Bhatt S. 2020. Estimating

495   the effects of non-pharmaceutical interventions on COVID-19 in Europe. *Nature*.

496   10.1038/s41586-020-2405-7

497   18. Kramer SC, and Shaman J. 2019. Development and validation of influenza forecasting for 64

498   temperate and tropical countries. *PLoS Comput Biol* 15:e1006742. 10.1371/journal.pcbi.1006742

499   19. Belgian institute for health (sciensano), access date: 6 july 2020 [Internet]. Available from:

500   https://epistat.wiv-isp.be/Covid/

501   20. Dipartimento della Protezione Civile,. COVID-19 italia-monitoraggio della situazione, date

502   of access: 6 july 2020 [Internet]. Available from: https://github.com/pcm-dpc/COVID-

503   19/tree/master/dati-andamento-nazionale

504   21. DATADISTA. Date of access: 6 july 2020 [Internet]. Available from:

505   https://github.com/datadista/datasets/tree/master/COVID 19

506   22. European Centre for Disease Prevention and Control. Geographic distribution of covid-19

507   cases worldwide, access date: 6 july 2020 [Internet]. Available from:

508   https://www.ecdc.europa.eu/en/publications-data/download-todays-data-geographic-distribution-

509   covid-19-cases-worldwide

510 23. Keeling MJ, Rohani P. Modeling infectious diseases in humans and animals [Internet].

511 Princeton: Princeton University Press; 2008. Available from:

512 http://www.loc.gov/catdir/toc/fy0805/2006939548.html

513 24. Lloyd AL. 2001. Destabilization of epidemic models with the inclusion of realistic

514 distributions of infectious periods. *Proc Biol Sci* 268:985-993. 10.1098/rspb.2001.1599

515 25. Wearing HJ, Rohani P, and Keeling MJ. 2005. Appropriate models for the management of

516 infectious diseases. *PLoS Med* 2:e174. 10.1371/journal.pmed.0020174

517 26. Li R, Pei S, Chen B, Song Y, Zhang T, Yang W, and Shaman J. 2020. Substantial

518 undocumented infection facilitates the rapid dissemination of novel coronavirus (SARS-CoV2).

519 *Science*. 10.1126/science.abb3221

520 27. Bi Q, Wu Y, Mei S, Ye C, Zou X, Zhang Z, Liu X, Wei L, Truelove SA, Zhang T, Gao W,

521 Cheng C, Tang X, Wu X, Wu Y, Sun B, Huang S, Sun Y, Zhang J, Ma T, Lessler J, and Feng T.

522 2020. Epidemiology and transmission of COVID-19 in 391 cases and 1286 of their close

523 contacts in Shenzhen, China: a retrospective cohort study. *Lancet Infect Dis*. 10.1016/S1473-

524 3099(20)30287-5

525 28. Verity R, Okell LC, Dorigatti I, Winskill P, Whittaker C, Imai N, Cuomo-Dannenburg G,

526 Thompson H, Walker PGT, Fu H, Dighe A, Griffin JT, Baguelin M, Bhatia S, Boonyasiri A,

527 Cori A, Cucunubá Z, FitzJohn R, Gaythorpe K, Green W, Hamlet A, Hinsley W, Laydon D,

528 Nedjati-Gilani G, Riley S, van Elsland S, Volz E, Wang H, Wang Y, Xi X, Donnelly CA, Ghani

529 AC, and Ferguson NM. 2020. Estimates of the severity of coronavirus disease 2019: a model-

530 based analysis. *Lancet Infect Dis*. 10.1016/S1473-3099(20)30243-7

531 29. Khalili M, Karamouzian M, Nasiri N, Javadi S, Mirzazadeh A, and Sharifi H. 2020.

532 Epidemiological characteristics of COVID-19: a systematic review and meta-analysis. *Epidemiol*

533 *Infect* 148:e130. 10.1017/S0950268820001430

534 30. Tindale LC, Stockdale JE, Coombe M, Garlock ES, Lau WYV, Saraswat M, Zhang L, Chen

535 D, Wallinga J, and Colijn C. 2020. Evidence for transmission of COVID-19 prior to symptom

536 onset. *Elife* 9. 10.7554/eLife.57149

537 31. Salje H, Tran Kiem C, Lefrancq N, Courtejoie N, Bosetti P, Paireau J, Andronico A, Hozé N,

538 Richet J, Dubost C-L, Le Strat Y, Lessler J, Levy-Bruhl D, Fontanet A, Opatowski L, Boelle P-

539 Y, and Cauchemez S. 2020. Estimating the burden of SARS-CoV-2 in France. *Science*.

540 10.1126/science.abc3517

541 32. O'Driscoll M, Ribeiro Dos Santos G, Wang L, Cummings DAT, Azman AS, Paireau J,

542 Fontanet A, Cauchemez S, and Salje H. 2021. Age-specific mortality and immunity patterns of

543 SARS-CoV-2. *Nature* 590:140-145. 10.1038/s41586-020-2918-0

544 33. Pastor-Barriuso R, Pérez-Gómez B, Hernán MA, Pérez-Olmeda M, Yotti R, Oteo-Iglesias J,

545 Sanmartín JL, León-Gómez I, Fernández-García A, Fernández-Navarro P, Cruz I, Martín M,

546 Delgado-Sanz C, Fernández de Larrea N, León Paniagua J, Muñoz-Montalvo JF, Blanco F,

547 Larrauri A, Pollán M, and ENE-COVID Study Group. 2020. Infection fatality risk for SARS-

548 CoV-2 in community dwelling population of Spain: nationwide seroepidemiological study. *BMJ*

549 371:m4509. 10.1136/bmj.m4509

550 34. King AA, Domenech de Cellès M, Magpantay FMG, and Rohani P. 2015. Avoidable errors

551 in the modelling of outbreaks of emerging pathogens, with special reference to Ebola. *Proc Biol*

552 *Sci* 282:20150347. 10.1098/rspb.2015.0347

553   35. He D, Ionides EL, and King AA. 2010. Plug-and-play inference for disease dynamics:

554   measles in large and small populations as a case study. *J R Soc Interface* 7:271-283.

555   10.1098/rsif.2009.0151

556   36. Althouse BM, Wenger EA, Miller JC, Scarpino SV, Allard A, Hébert-Dufresne L, and Hu H.

557   2020. Superspreading events in the transmission dynamics of SARS-CoV-2: Opportunities for

558   interventions and control. *PLoS Biol* 18:e3000897. 10.1371/journal.pbio.3000897

559   37. Kain MP, Childs ML, Becker AD, and Mordecai EA. 2020. Chopping the tail: How

560   preventing superspreading can help to maintain COVID-19 control. *Epidemics* 34:100430.

561   10.1016/j.epidem.2020.100430

562   38. Lloyd-Smith JO, Schreiber SJ, Kopp PE, and Getz WM. 2005. Superspreading and the effect

563   of individual variation on disease emergence. *Nature* 438:355-359. 10.1038/nature04153

564   39. Endo A, Centre for the Mathematical Modelling of Infectious Diseases COVID-19 Working

565   Group, Abbott S, Kucharski AJ, and Funk S. 2020. Estimating the overdispersion in COVID-19

566   transmission using outbreak sizes outside China. *Wellcome Open Res* 5:67.

567   10.12688/wellcomeopenres.15842.3

568   40. Alimohamadi Y, Taghdir M, and Sepandi M. 2020. Estimate of the Basic Reproduction

569   Number for COVID-19: A Systematic Review and Meta-analysis. *J Prev Med Public Health*

570   53:151-157. 10.3961/jpmph.20.076

571   41. Ionides EL, Nguyen D, Atchadé Y, Stoev S, and King AA. 2015. Inference for dynamic and

572   latent variable models via iterated, perturbed Bayes maps. *Proc Natl Acad Sci U S A* 112:719-

573   724. 10.1073/pnas.1410597112

574   42. King AA, Nguyen D, Ionides EL. Statistical inference for partially observed markov

575   processes via the r package pomp. Journal of Statistical Software. 2016;69(1):1–43.

576   43. R Core Team. R: A language and environment for statistical computing [Internet]. Vienna,

577   Austria: R Foundation for Statistical Computing; 2020. Available from: https://www.R-

578   project.org/

579   44. de Vries A, Microsoft. Checkpoint: Install packages from snapshots on the checkpoint server

580   for reproducibility [Internet]. 2020. Available from: https://CRAN.R-

581   project.org/package=checkpoint

582   45. Raue A, Kreutz C, Maiwald T, Bachmann J, Schilling M, Klingmüller U, and Timmer J.

583   2009. Structural and practical identifiability analysis of partially observed dynamical models by

584   exploiting the profile likelihood. *Bioinformatics* 25:1923--1929.

585   46. Domenech de Cellès M, Magpantay FMG, King AA, and Rohani P. 2018. The impact of past

586   vaccination coverage and immunity on pertussis resurgence. *Sci Transl Med* 10.

587   10.1126/scitranslmed.aaj1748

588   47. Domenech de Cellès M, Arduin H, Lévy-Bruhl D, Georges S, Souty C, Guillemot D, Watier

589   L, and Opatowski L. 2019. Unraveling the seasonal epidemiology of pneumococcus. *Proc Natl*

590   *Acad Sci U S A* 116:1802-1807. 10.1073/pnas.1812388116

591   48. Maier BF, and Brockmann D. 2020. Effective containment explains subexponential growth

592   in recent confirmed COVID-19 cases in China. *Science* 368:742-746. 10.1126/science.abb4557

593   49. Pollán M, Pérez-Gómez B, Pastor-Barriuso R, Oteo J, Hernán MA, Pérez-Olmeda M,

594   Sanmartín JL, Fernández-García A, Cruz I, Fernández de Larrea N, Molina M, Rodríguez-

595   Cabrera F, Martín M, Merino-Amador P, León Paniagua J, Muñoz-Montalvo JF, Blanco F, Yotti

596   R, and ENE-COVID Study Group. 2020. Prevalence of SARS-CoV-2 in Spain (ENE-COVID): a

597   nationwide, population-based seroepidemiological study. *Lancet*. 10.1016/S0140-

598   6736(20)31483-5

599   50. Kucharski AJ, Russell TW, Diamond C, Liu Y, Edmunds J, Funk S, Eggo RM, and Centre

600   for Mathematical Modelling of Infectious Diseases COVID-19 working group. 2020. Early

601   dynamics of transmission and control of COVID-19: a mathematical modelling study. *Lancet*

602   *Infect Dis*. 10.1016/S1473-3099(20)30144-4

603   51. Davies NG, Klepac P, Liu Y, Prem K, Jit M, CMMID COVID-19 working group, and Eggo

604   RM. 2020. Age-dependent effects in the transmission and control of COVID-19 epidemics. *Nat*

605   *Med*. 10.1038/s41591-020-0962-9

606   52. Bunyavanich S, Do A, and Vicencio A. 2020. Nasal Gene Expression of Angiotensin-

607   Converting Enzyme 2 in Children and Adults. *JAMA*. 10.1001/jama.2020.8707

608   53. Jüni P, Rothenbühler M, Bobos P, Thorpe KE, da Costa BR, Fisman DN, Slutsky AS, and

609   Gesink D. 2020. Impact of climate and public health interventions on the COVID-19 pandemic:

610   a prospective cohort study. *CMAJ* 192:E566-E573. 10.1503/cmaj.200920

611   54. Gaudart J, Landier J, Huiart L, Legendre E, Lehot L, Bendiane MK, Chiche L, Petitjean A,

612   Mosnier E, Kirakoya-Samadoulougou F, Demongeot J, Piarroux R, and Rebaudet S. 2021.

613   Factors associated with the spatial heterogeneity of the first wave of COVID-19 in France: a

614   nationwide geo-epidemiological study. *Lancet Public Health*. 10.1016/S2468-2667(21)00006-2

615   55. Sehra ST, Salciccioli JD, Wiebe DJ, Fundin S, and Baker JF. 2020. Maximum Daily

616   Temperature, Precipitation, Ultraviolet Light, and Rates of Transmission of Severe Acute

617   Respiratory Syndrome Coronavirus 2 in the United States. *Clin Infect Dis* 71:2482-2487.

618   10.1093/cid/ciaa681

619   56. Baker RE, Yang W, Vecchi GA, Metcalf CJE, and Grenfell BT. 2020. Susceptible supply

620   limits the role of climate in the early SARS-CoV-2 pandemic. *Science* 369:315-319.

621   10.1126/science.abc2535

622   57. Park SW, Cornforth DM, Dushoff J, and Weitz JS. 2020. The time scale of asymptomatic

623   transmission affects estimates of epidemic potential in the COVID-19 outbreak. *Epidemics*

624   31:100392. 10.1016/j.epidem.2020.100392

625   58. Dee K, Goldfarb DM, Haney J, Amat JAR, Herder V, Stewart M, Szemiel AM, Baguelin M,

626   and Murcia PR. 2021. Human rhinovirus infection blocks SARS-CoV-2 replication within the

627   respiratory epithelium: implications for COVID-19 epidemiology. *J Infect Dis*.

628   10.1093/infdis/jiab147

629   59. Ozaras R, Cirpin R, Duman H, Duran A, Arslan O, and Leblebicioglu H. 2020. An open call

630   for influenza vaccination pending the new wave of COVID-19. *J Med Virol*. 10.1002/jmv.26272

631   60. Lessler J, Reich NG, Brookmeyer R, Perl TM, Nelson KE, and Cummings DAT. 2009.

632   Incubation periods of acute respiratory viral infections: a systematic review. *Lancet Infect Dis*

633   9:291-300. 10.1016/S1473-3099(09)70069-6

634   61. Carrat F, Vergu E, Ferguson NM, Lemaitre M, Cauchemez S, Leach S, and Valleron A-J.

635   2008. Time lines of infection and disease in human influenza: a review of volunteer challenge

636   studies. *Am J Epidemiol* 167:775-785. 10.1093/aje/kwm375

637   62. Kim D, Quinn J, Pinsky B, Shah NH, and Brown I. 2020. Rates of Co-infection Between

638   SARS-CoV-2 and Other Respiratory Pathogens. *JAMA*. 10.1001/jama.2020.6266

639   63. Marín-Hernández D, Schwartz RE, and Nixon DF. 2020. Epidemiological evidence for

640   association between higher influenza vaccine uptake in the elderly and lower COVID-19 deaths

641   in Italy. *J Med Virol*. 10.1002/jmv.26120

642   64. Arokiaraj MC. 2020. Correlation of Influenza Vaccination and the COVID-19 Severity.

643   *Available at SSRN 3572814*.

644   65. Del Riccio M, Lorini C, Bonaccorsi G, Paget J, and Caini S. 2020. The Association between

645   Influenza Vaccination and the Risk of SARS-CoV-2 Infection, Severe Illness, and Death: A

646   Systematic Review of the Literature. *Int J Environ Res Public Health* 17.

647   10.3390/ijerph17217870

648   66. Salem ML, and El-Hennawy D. 2020. The possible beneficial adjuvant effect of influenza

649   vaccine to minimize the severity of COVID-19. *Med Hypotheses* 140:109752.

650   10.1016/j.mehy.2020.109752

651   67. Pinky L, Dobrovolny HM. SARS-CoV-2 coinfections: Could influenza and the common

652   cold be beneficial? J Med Virol. 2020 May;.

653   68. Paget J, Caini S, Cowling B, Esposito S, Falsey AR, Gentile A, Kyncl J, McIntyre C, Pitman

654   R, and Lina B. 2020. The impact of influenza vaccination on the COVID-19 pandemic?

655   Evidence and lessons for public health policies. *Vaccine*. 10.1016/j.vaccine.2020.08.024

656   69. Domenech de Cellès M, Arduin H, Varon E, Souty C, Boëlle P-Y, Lévy-Bruhl D, van der

657   Werf S, Soulary J-C, Guillemot D, Watier L, and Opatowski L. 2018. Characterizing and

658   Comparing the Seasonality of Influenza-Like Illnesses and Invasive Pneumococcal Diseases

659   Using Seasonal Waveforms. *Am J Epidemiol* 187:1029-1039. 10.1093/aje/kwx336

660   70. Camacho A, Ballesteros S, Graham AL, Carrat F, Ratmann O, and Cazelles B. 2011.

661   Explaining rapid reinfections in multiple-wave influenza outbreaks: Tristan da Cunha 1971

662   epidemic as a case study. *Proc Biol Sci* 278:3635-3643. 10.1098/rspb.2011.0300

663   71. Svensson A. 2007. A note on generation times in epidemic models. *Math Biosci* 208:300-

664   311. 10.1016/j.mbs.2006.10.010

665   72. Wood SN. 2010. Statistical inference for noisy nonlinear ecological dynamic systems. *Nature*

666   466:1102-1104. 10.1038/nature09319

667

Figure 1

Potential drivers of SARS-CoV-2 transmission in Belgium, Italy, Norway, and Spain.

A: time plot of the stringency index, a country-level aggregate measure of the number and of the strictness of non-pharmaceutical control measures implemented by governments. The vertical dashed line indicates the start of the nationwide lockdown [17]. B: time plot of influenza incidence, calculated as the product of the incidence of influenza-like illnesses and of the fraction of samples positive to any influenza virus (see also Fig. S1 for a time plot of the latter two variables). The vertical dashed lines delimitate the period of overlap between SARS-CoV-2and influenza, defined as the period between the assumed start date of SARS-CoV- 2 community transmission and 6 weeks after the epidemic peak of influenza[68]. In each country, the time series displayed were incorporated as covariates, which modulated the transmission rate of SARS-CoV-2 in our model (see Methods). In B, the *y*-axis values differ for each panel.

A

Belgium

Italy

Norway

Spain

Stringency index

Time (days, year 2020)

B

Belgium

Italy

Norway

Spain

Incidence rate of influenza (per 100,000 per week)

Time (days, year 2020)
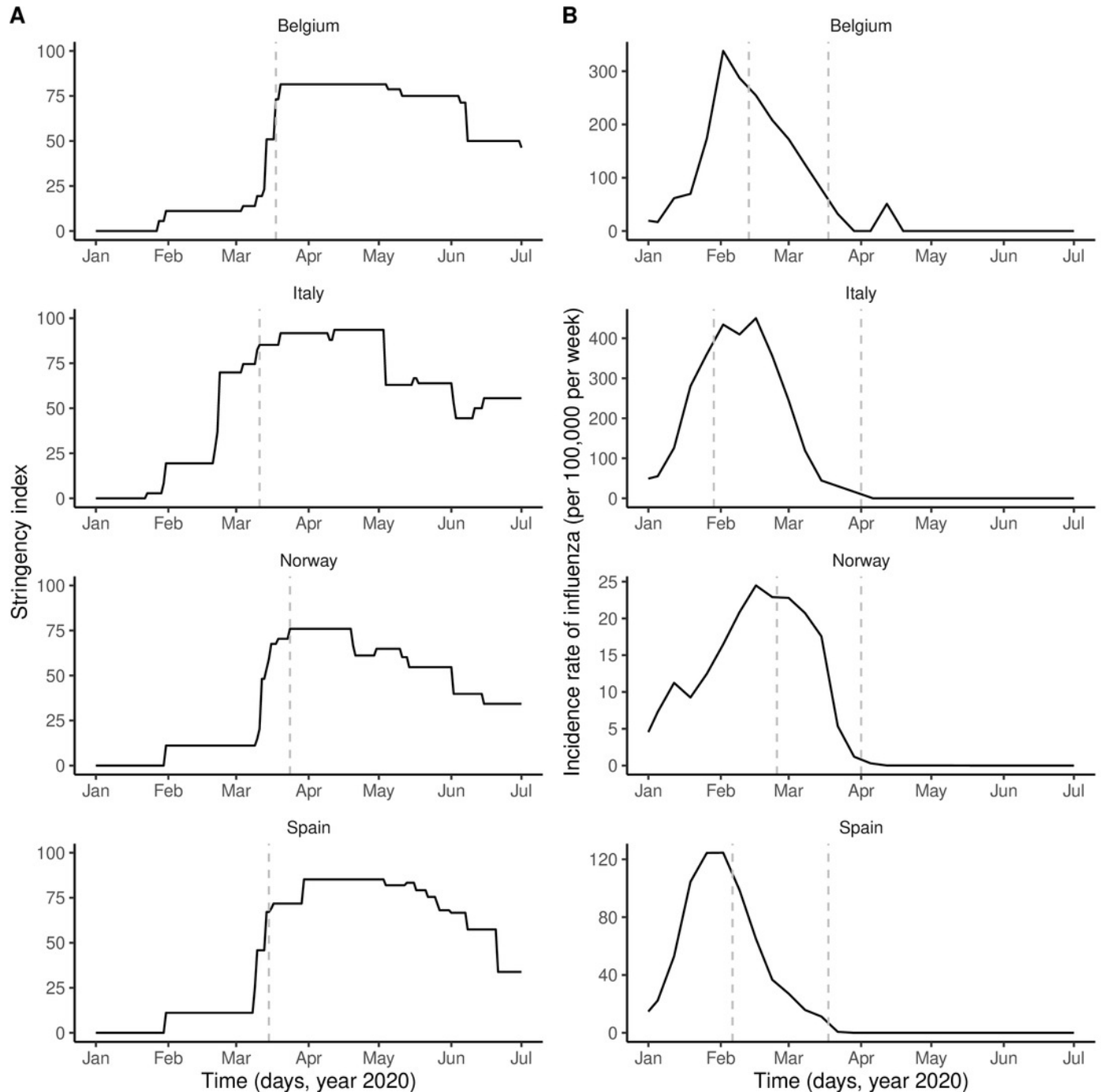
Figure 2

Dynamics of SARS-CoV-2 transmission and of COVID-19 mortality in Belgium, Italy, Norway, and Spain.

A: time plot of the estimated effective reproductive number (Re). In each panel, the black line represents the maximum likelihood estimate and the grey ribbon the 95% confidence interval (calculated based on the likelihood profile of the influenza impact parameter, cf. Table2) in each country. The dotted black line represents the effective reproduction number estimated from a model without influenza (i.e., with the influenza impact parameter fixed to 0 and the other parameters estimated from the data). The horizontal grey line is at Re = 1. B: time plot of the simulated and observed numbers of daily deaths caused by SARS-CoV-2. In each panel, the light grey lines represent 1,000 model simulations at the maximum likelihood estimate, with one simulation highlighted in dark grey; the black line represents the actual death counts. In A and B, the *x*-axis and the *y*-axis values differ for each panel.

A

Belgium

Italy

Norway

Spain

Effective reproduction number

Time (days, year 2020)

B

Belgium

Italy

Norway

Spain

Daily deaths

Time (days, year 2020)
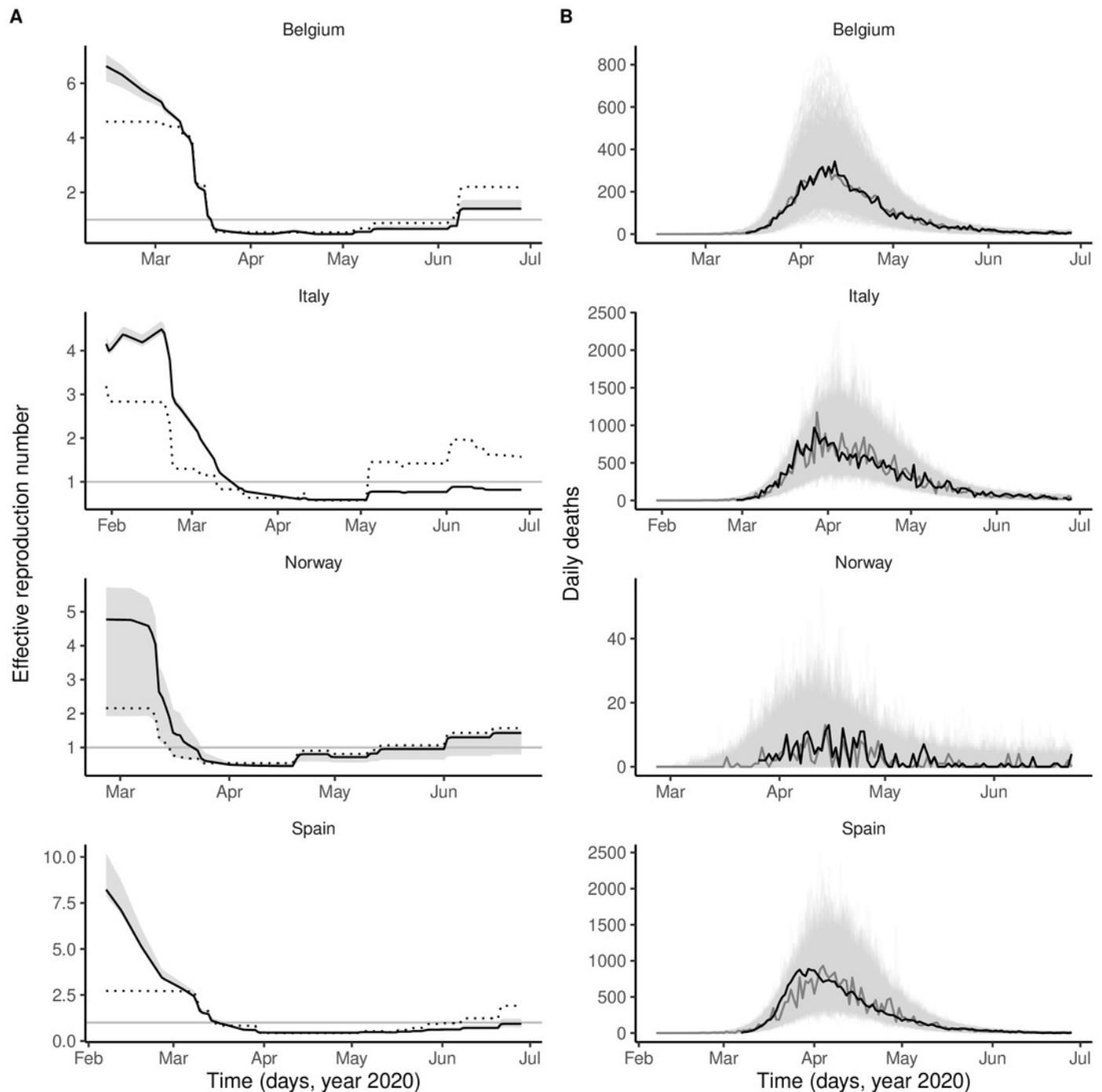
List of model parameters.

Symbol	Meaning	Fixed value or estimation range	Comment/Source
$D_E = 1/\sigma$	Average latent period	4 days	[26]
$D_I = 1/\sigma$	Average infectious period	5 days	Fixed to have average generation time of 6.5 days. Sensitivity analyses: 2,7days
$T_g = D_E + D_I/2$	Average generation time	6.5 days	[17, 27]
$1/\kappa$	Average onset-to-death time	17.8 days	[28, 17] Sensitivity analysis: 13 days
μ	Infection- fatality ratio	0.01	[17, 32] Sensitivity analysis: 0.005
N	Population size	Belgium: 11.50 M; Italy: 60.32 M; Norway: 5.37 M; Spain: 47.01M	2019 demographic data from the World Bank
$si(t)$	Stringency index	fixed (covariate)	Fig. 1A
$F(t)$	Incidence of influenza (rescaled)	fixed (covariate)	Fig. 1B
R_0	Basic reproduction number	1–10	[40]
b	Impact of non-pharmaceutical control measures	0.5–2	[17]
β_F	Impact of flu on SARS-CoV-2 transmission	$\mathbb{R}$	
k	Dispersion of individual reproduction number	0.16	[37, 39]
k_D	Over-dispersion in death reporting	$\mathbb{R}^+$	
$E_1(0)$	Initial no exposed	0–10^4	Initial condition

Model parameter estimates in Belgium, Italy, Norway, and Spain.

For the proportion infected as of May 4, the numbers between parentheses represent a 95% prediction interval, based on 1,000 simulations at the maximum likelihood estimate. For the other parameters, they represent an approximate 95% confidence interval, calculated using either the profile likelihood[45] (parameter beta_F) or a parametric bootstrap (other parameters). SE: standard error, calculated using 5 replicate particle filters, each with 20,000 particles, at the maximum likelihood estimate.

Quantity	Belgium	Italy	Norway	Spain
Study period (year 2020)	13 Feb–28 Jun	29 Jan–28 Jun	25 Feb–28 Jun	06 Feb–28 Jun
Log-likelihood (SE)	−384.4 (<0.1)	−649.5 (0.1)	−161.8 (<0.1)	−558.5 (0.2)
Basic reproduction number (R_0)	3.4 (2.5, 4.1)	1.2 (1.1, 1.4)	2.2 (1.0, 2.5)	1.4 (1.0, 1.9)
Impact of control measures (b)	1.03 (0.96, 1.07)	0.53 (0.50, 0.61)	1.05 (0.53, 1.08)	0.75 (0.56, 0.86)
Average relative variation in SARS-CoV-2 transmission rate associated with influenza (β_F)	0.8 (0.5, 1.3)	1.8 (1.5, 2.0)	1.0 (0.1, 2.0)	2.4 (1.7, 4.0)
Initial number exposed to SARS-CoV-2 ($E_1(0)$)	100 (20, 200)	530 (260, 1000)	130 (100, 2800)	400 (170, 780)
Over-dispersion in death reporting (k_D)	7×10^{-4} (1,47) $\times$ 10^{-4}	0.07 (0.05, 0.09)	0.16 (0.01, 0.42)	0.08 (0.05, 0.10)
Proportion infected, as of 4 May 2020 (%)	8.8 (3.7, 17.1)	5.4 (3.9, 7.3)	0.4 (0.2, 0.8)	6.0 (3.8, 8.6)